

Simple Self-Organizing Map with Visual Transformer

Alan Luo, Kaiwen Yuan

Abstract—Vision Transformers (ViTs) have demonstrated exceptional performance in various vision tasks. However, they tend to underperform on smaller datasets due to their inherent lack of inductive biases. Current approaches address this limitation implicitly—often by pairing ViTs with pretext tasks or by distilling knowledge from convolutional neural networks (CNNs) to strengthen the prior. In contrast, Self-Organizing Maps (SOMs), a widely adopted self-supervised framework, are inherently structured to preserve topology and spatial organization, making them a promising candidate to directly address the limitations of ViTs in limited or small training datasets. Despite this potential, equipping SOMs with modern deep learning architectures remains largely unexplored. In this study, we conduct a novel exploration on how Vision Transformers (ViTs) and Self-Organizing Maps (SOMs) can empower each other, aiming to bridge this critical research gap. Our findings demonstrate that these architectures can synergistically enhance each other, leading to significantly improved performance in both unsupervised and supervised tasks. Code will be publicly available.

Index Terms—Unsupervised learning, Self-organizing Map, Visual Transformer

I. INTRODUCTION

The recent success of transformer architecture [1] in natural language processing (NLP) has quickly inspired the vision community to rethink vision tasks [2], [3] in a similar way. The Vision Transformer (ViT), introduced by [2], marks a significant shift in the paradigm of computer vision, transitioning from convolutional neural networks (CNNs) towards transformer-based architectures. Conventionally, ViTs model images as sequences of patches, analogous to the concept of tokens in NLP. This approach has demonstrated competitive performance on image classification tasks when compared to traditional CNNs, especially when pre-trained on large-scale datasets. However, a well-documented limitation of ViTs is their lack of inductive biases [2], resulting in poor performance when trained on limited or small training datasets. Various effective techniques [4], [5] have been proposed to address this challenge implicitly by learning strong priors, including methods such as pretext tasks [4], [5] or knowledge distillation [6]. While these approaches are effective, their lack of inherent inductive biases presents an opportunity to explore new methods for directly embedding such biases into ViTs.

On the other hand, self-organizing maps (SOMs) [7], a powerful self-supervised method, can intrinsically preserve topology and spatial organization as inductive biases, posing

Alan Luo is with the School of Computer, Data & Information Sciences (CDIS) at the University of Wisconsin-Madison, 1210 W Dayton St, Madison, WI 53706, USA (e-mail: aluo7@wisc.edu).

Kaiwen is with Safari AI Inc., 12 E 49th St. New York, NY 10017, USA (e-mail: kaiwen.yuan@getsafari.ai).

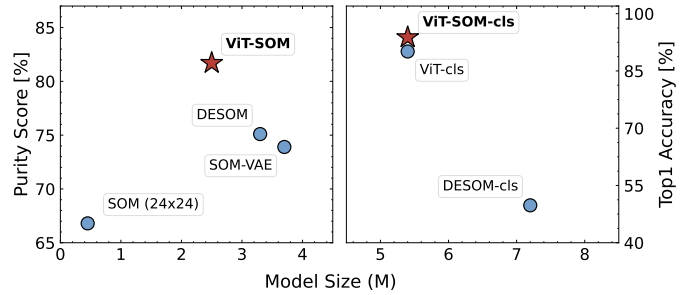


Fig. 1. Model size and task performances comparisons between ViT-SOM and existing methods on F-MNIST and CIFAR-10 datasets.

a natural solution to address the challenges posed by ViTs. However, while SOMs have been widely adopted in various data analysis applications [8], [9] over the past decades, classic SOMs suffer from a major limitation: poor feature abstraction capabilities. As such, ViTs serve as a strong complement to SOMs, addressing their weakness in feature abstraction while benefiting from SOMs inherent inductive biases.

While this hypothesis is promising, the prevailing research in the field has yet to explore this direction. The only related work we are aware of is TENSO [10], which focuses on low-dimensional trajectory data. The majority of relevant publications have focused on various CNN based architectures or variants [11], [12], [13], [14], [15], [16] to enhance SOMs feature extraction. For example, one pioneering work, DSOM [12], demonstrated a significant 7.17% performance improvement over classic SOMs on the MNIST dataset. More recent works have focused on handling sequential data with Long Short-Term Memory (LSTM) [15], [17] and Contrastive Predictive Coding (CPC) [18], rather than leveraging more powerful architectures like ViTs.

Therefore, there is a clear research gap in studying the underexplored, mutually beneficial interactions between SOMs and ViTs. In our work, we propose ViT-SOM, a novel framework that integrates ViTs with SOMs to leverage the strengths of both architectures. Our approach involves two steps: 1) evaluating the unsupervised setting, similar to [14], [16], for clustering tasks on various datasets; 2) extending the experiments to supervised classification on small datasets. As detailed in later sections, our simple yet effective method leads to performance improvements in both settings on various benchmark datasets. We believe our work can serve as a strong foundation to initiate this innovative research direction.

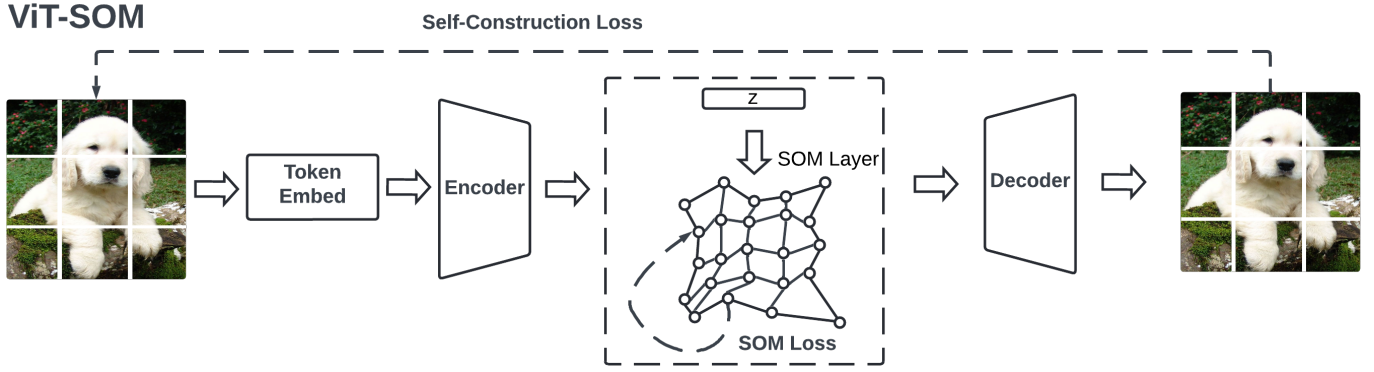


Fig. 2. ViT-SOM architecture.

II. PROPOSED METHOD

A. SOM Debrief

SOMs utilize a competitive learning strategy, where each unit—often referred to as a prototype or neuron—competes to represent the input data. For a given input z and a weight matrix W_{som} , the best matching unit (BMU) is identified at each cycle based on spatial distance. Once the BMU is determined, the weights are adjusted according to its distance to each input example, typically considering both spatial distance and learning rate (with decay). A naive SOM update process from step k to $k+1$ can be described as follows:

$$W_{som,k+1} = W_{som,k} + \alpha_k \cdot h_{k,i,j}(z, W_{som,k}) \quad (1)$$

where α_k is the learning rate and $h_{k,i,j}$ denotes the neighborhood (update) function at step k between the BMU j and an arbitrary neuron i . In practice [16], a common approach to the neighborhood function $h_{k,a,b}$ is to employ a Gaussian neighborhood function with a distance metric between two neurons:

$$h_{k,i,j} = \exp\left(-\frac{\sum_{i=1}^n d_{ij}}{2T(k)^2}\right) \quad (2)$$

where $T(k)$, often termed temperature, decays with time, and d_{ij} represents the distance metric between the BMU and an arbitrary neuron.

B. ViT-SOM

Classical SOMs update prototypes sequentially [19], which is computationally inefficient and incompatible with GPU parallelization. To address this, we adopt a batch-compatible framework [16], where BMUs for all samples are computed in parallel. This strategy accelerates training by fixing or periodically updating BMU assignments, enabling parallel processing of batches. Prototypes are then optimized via backpropagation on the loss:

$$L_{som} = \frac{1}{N} \sum_{i=1}^N \sum_{j=1}^M w_{ij} \cdot d_{ij}(z) \quad (3)$$

where z is the input data point (in our context, an embedding space element), N is the number of input samples, M is the number of SOM units, w_{ij} represents the weight based on

the distance to the BMU, and d_{ij} is the distance between input sample i and SOM unit j . Despite their uncontested use in typical SOM architectures [14], [16], both the Euclidean and Manhattan distance functions suffer largely from scale variance. To address this limitation, we instead apply cosine similarity for d_{ij} :

$$d_{ij}(z) = 1 - \frac{z \cdot w_{ij}}{\|z\| \|w_{ij}\|} \quad (4)$$

By leveraging its scale invariance and angular alignment, cosine similarity better captures fine-grained relationships between vectors in high-dimensional spaces, enabling the SOM to more accurately constrain the latent topology.

Figure II demonstrates the architecture of ViT-SOM, compared with the classic ViT. The major difference lies in the embedding layer. Instead of naively passing the embedding vector z to the decoder, ViT-SOM introduces an SOM layer to self-supervise the embedding vector for topology-preserving training:

$$J = \sum_{z \in \mathcal{Z}} \min_{i,j,N} \left(1 - \frac{z \cdot w_{ij}}{\|z\| \|w_{ij}\|}\right) \quad (5)$$

Since the SOM has a grid topology, this formulation ensures that the embedding vector z is spatially projected onto the BMUs, preserving the topology during each training iteration. As training proceeds, the continuous update of $z \in \mathcal{Z}$ via neighborhood updates helps in creating a smooth and ordered mapping from the embedding space to the grid. This iterative process minimizes training errors while also enforcing topological consistency across the grid, ultimately leading to enhanced feature representation and improved data organization.

We utilize a tiny version of the Vision Transformer (ViT) [20], with detailed configurations for clustering and classification provided in Table I. For the SOM layer, we adopt a standard self-organizing map governed by Equations 2 and 3. Prototype updates are computed in batches, with temperature $T(k)$ decaying exponentially from T_{\max} to T_{\min} for training iterations $k = 1, \dots, K$. This fine-grained decay schedule ensures stable quantization and effective clustering throughout training, as smaller, more frequent adjustments to $T(k)$ reduce noise in prototype updates and stabilize learning. In both

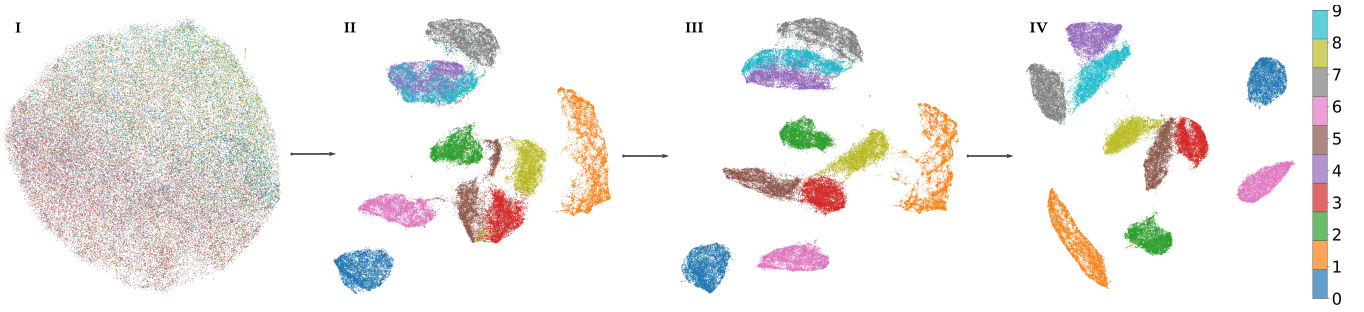


Fig. 3. UMAP visualization of latent space embeddings from ViT-SOM model training progression on MNIST. Projections shown at epochs 0, 25, 50, 200. Color mapping represents ground truth classes, demonstrating emergent cluster separation during training.

TABLE I
ViT BACKBONE CONFIGURATIONS FOR ViT-SOM ON CLASSIFICATION
AND CLUSTERING TASKS.

Task	Embed. Dim.	MLP Dim.	Enc./Dec. Depth	Heads	Params
Classification	192	768	12 / 2	3	5.4M
Clustering	16	64	4 / 2	2	2.5M

supervised and unsupervised settings, the objective functions are weighted by λ :

$$L_{total} = \lambda \cdot L_{som} + L_{nn} \quad (6)$$

where L_{nn} is the loss of the deep neural networks.

III. EXPERIMENTS AND RESULTS

A. Training

The pipeline is implemented in Pytorch and a single NVIDIA RTX 4090 GPU is used for training. AdamW [21] is employed as the optimizer with an initial learning rate of $lr = 0.0005$, decayed via cosine annealing, and hyperparameters $\beta_1 = 0.9$, $\beta_2 = 0.999$ for all configurations. For classification tasks, standard data augmentations are applied to improve generalization. For clustering tasks, no data augmentation is used (e.g., random cropping, flipping, and color jitter). All models are trained from scratch, and no pre-trained weights are used during initialization.

B. Datasets.

a) Unsupervised: We evaluate our unsupervised learning experiments on the MNIST [22], Fashion-MNIST [23], and USPS [24] datasets so that we can fairly compare with DESOMs settings [16]. The MNIST dataset consists of 70,000 28×28 grayscale images of handwritten digits (0-9), split into 60,000 training images and 10,000 testing images. Fashion-MNIST includes 70,000 grayscale images of fashion items across 10 categories, with a similar train-test split. The USPS dataset contains 9,298 16×16 grayscale images of handwritten digits (0-9).

b) Supervised: For classification tasks, we evaluate model performance on small natural image datasets, including CIFAR-10, CIFAR-100 [25], Flowers17 [26], and SVHN [27]. Both CIFAR-10 and CIFAR-100 contain 60,000 32×32 color images, with CIFAR-10 spanning 10 classes and CIFAR-100 offering a more granular classification challenge across 100 classes. Flowers17 comprises 1,360 color images of flowers across 17 categories (80 images per class), making it suitable for fine-grained classification tasks. The SVHN dataset provides 32×32 color images of house numbers from street view imagery, organized into 10 classes.

C. Unsupervised Clustering Results

The widely recognized purity score metric is adopted to evaluate the clustering performance across datasets. Table II presents clustering benchmark results for various SOM-equipped models, including SOM-VAE [14], DESOM [16], and our proposed ViT-SOM. ViT-SOM achieves significantly higher purity scores on MNIST and Fashion-MNIST compared to SOM-VAE while using fewer learnable parameters. Notably, ViT-SOM outperforms DESOM—a CNN-based variant—across all datasets with 24% fewer parameters and an average improvement of 12.5% in purity scores, demonstrating ViTs’ strength as a feature extractor in SOM frameworks.

Figure 3 visualizes the evolution of the ViT-encoded latent space via UMAP projections during early-stage training. As training progresses, the ViT-SOM objective drives embeddings to form well-separated clusters, with points colored by digit class coalescing into distinct groups. This demonstrates the capability of our proposed method to organize latent representations semantically. Figure 4 further validates this organization by decoding the SOM prototypes into a 24×24 grid. Here, semantically similar digits—such as (6 and 0), (4, 7, and 9), or (3, 8, and 2)—are topologically grouped as neighbors, reflecting the latent space structure observed in the UMAP.

While the majority of prototypes align with semantic groupings, a small subset (e.g., ambiguous 5s surrounded by 3s and 0s) highlights limitations inherent to SOMs. These artifacts arise from sensitivity to initialization and the fixed grid structure, which can trap prototypes in suboptimal regions of the latent space. Future work could explore adaptive grid

- ance for improving vision transformers on tiny datasets,” in *European Conference on Computer Vision*. Springer, 2022, pp. 110–127.
- [7] T. Kohonen, “Self-organized formation of topologically correct feature maps,” *Biological cybernetics*, vol. 43, no. 1, pp. 59–69, 1982.
 - [8] H. Wirth, M. Löffler, M. von Bergen, and H. Binder, “Expression cartography of human tissues using self organizing maps,” *Nature precedings*, pp. 1–1, 2011.
 - [9] R. Wang, T. Shi, X. Zhang, J. Wei, J. Lu, J. Zhu, Z. Wu, Q. Liu, and M. Liu, “Implementing in-situ self-organizing maps with memristor crossbar arrays for data mining and optimization,” *Nature communications*, vol. 13, no. 1, p. 2289, 2022.
 - [10] S. Yoon *et al.*, “Anomalous indoor human trajectory detection based on the transformer encoder and self-organizing map,” *IEEE Access*, vol. 11, pp. 131 848–131 865, 2023.
 - [11] P. Lichodziejewski, A. N. Zincir-Heywood, and M. I. Heywood, “Host-based intrusion detection using self-organizing maps,” in *Proceedings of the 2002 International Joint Conference on Neural Networks. IJCNN’02 (Cat. No. 02CH37290)*, vol. 2. IEEE, 2002, pp. 1714–1719.
 - [12] N. Liu, J. Wang, and Y. Gong, “Deep self-organizing map for visual classification,” in *2015 international joint conference on neural networks (IJCNN)*. IEEE, 2015, pp. 1–6.
 - [13] C. Ferles, Y. Papanikolaou, and K. J. Naidoo, “Denoising autoencoder self-organizing map (dasom),” *Neural Networks*, vol. 105, pp. 112–131, 2018.
 - [14] V. Fortuin, M. Hüser, F. Locatello, H. Strathmann, and G. Rätsch, “Somvae: Interpretable discrete representation learning on time series,” in *International Conference on Learning Representations (ICLR 2019)*. OpenReview. net, 2019.
 - [15] F. Forest, M. Lebbah, H. Azzag, and J. Lacaille, “Deep architectures for joint clustering and visualization with self-organizing maps,” in *Trends and Applications in Knowledge Discovery and Data Mining: PAKDD 2019 Workshops, BDM, DLKT, LDRC, PAISI, WeL, Macau, China, April 14–17, 2019, Revised Selected Papers 23*. Springer, 2019, pp. 105–116.
 - [16] F. Forest, M. Lebba, H. Azzag, and L. J., “Deep embedded self-organizing maps for joint representation learning and topology-preserving clustering,” *Neural Computing and Applications*, vol. 33, no. 24, pp. 17 439–17 469, 2021.
 - [17] L. Manduchi, M. Hüser, M. Faltys, J. Vogt, G. Rätsch, and V. Fortuin, “T-dpsom: An interpretable clustering method for unsupervised learning of patient health states,” in *Proceedings of the Conference on Health, Inference, and Learning*, 2021, pp. 236–245.
 - [18] I. A. Huijben, A. A. Nijdam, S. Overeem, M. M. Van Gilst, and R. Van Sloun, “Som-cpc: Unsupervised contrastive learning with self-organizing maps for structured representations of high-rate time series,” in *International Conference on Machine Learning*. PMLR, 2023, pp. 14 132–14 152.
 - [19] M. Cottrell, J.-C. Fort, and G. Pagès, “Theoretical aspects of the som algorithm,” *Neurocomputing*, vol. 21, no. 1-3, pp. 119–138, 1998.
 - [20] H. Touvron, M. Cord, M. Douze, F. Massa, A. Sablayrolles, and H. Jégou, “Training data-efficient image transformers & distillation through attention,” in *International Conference on Machine Learning*. PMLR, 2021, pp. 10 347–10 357.
 - [21] I. Loshchilov and F. Hutter, “Decoupled weight decay regularization,” in *International Conference on Learning Representations (ICLR)*, 2018.
 - [22] Y. LeCun, L. Bottou, Y. Bengio, and P. Haffner, “Gradient-based learning applied to document recognition,” in *Proceedings of the IEEE*. IEEE, 1998, pp. 2278–2324.
 - [23] H. Xiao, K. Rasul, and R. Vollgraf, “Fashion-mnist: A novel image dataset for benchmarking machine learning algorithms,” *Journal of Machine Learning Research*, vol. 18, no. 1, pp. 1–5, 2017.
 - [24] J. J. Hull, “A database for handwritten text recognition research,” *IEEE Transactions on Pattern Analysis and Machine Intelligence*, vol. 16, no. 5, pp. 550–554, 1994.
 - [25] A. Krizhevsky, “Learning multiple layers of features from tiny images,” University of Toronto, Tech. Rep., 2009.
 - [26] M.-E. Nilsback and A. Zisserman, “A visual vocabulary for flower classification,” in *IEEE Conference on Computer Vision and Pattern Recognition*, vol. 2, 2006, pp. 1447–1454.
 - [27] Y. Netzer, T. Wang, A. Coates, A. Bissacco, B. Wu, and A. Y. Ng, “Reading digits in natural images with unsupervised feature learning,” in *NIPS Workshop on Deep Learning and Unsupervised Feature Learning*, 2011. [Online]. Available: <http://ufldl.stanford.edu/housenumbers>
 - [28] W. Chen, W. Zhang, and W. Wang, “A multi-view convolutional neural network based on cross-connection and residual-wider,” *Applied Intelligence*, vol. 53, pp. 14 316–14 328, 2023. [Online]. Available: <https://link.springer.com/article/10.1007/s10489-022-04248-y>